



3-4-12

THE LOCAL EFFECT OF SOIL ON THE PROPAGATION OF SEISMIC WAVE

Pei-Lin Chen¹ and Yi-Min Keng²

^{1,2}Department of Civil Engineering, National Cheng Kung University,
Tainan, Taiwan, R. O. C.

SUMMARY

The objective of this study is to investigate the amplification effect of single layered soil medium. To obtain the amplification spectra, the generalized ray theory [1] [2] is employed to calculate the velocity responses in time domain, in which the source of shear force with sine-like time function is assumed, and the fundamental frequency is about 2.4 Hz in far field for the calculated amplification spectra, also the recorded strong ground motion and the calculated amplification spectra in SMART-1 array region [3] were used for comparison, from which we observed that the amplification effect was most obvious in the frequency range from 0.2 Hz to 1.5 Hz for SMART-1 array.

INTRODUCTION

As the fault slipped, the released energy, which propagated in the soil media, will be recorded on the ground surface. Since the signals received will be different for distinct media through which the seismic wave propagate, hence it is the main goal for us to study the amplification effect of soil medium, in which the seismic wave propagate. Generally speaking, the deeper media under the crust are composed of rock or other harder materials which will have little amplification effect on the propagation of seismic wave, however, the surface layer, due to its soft property, will amplify the signals of the propagating seismic wave. In site study, a large number of strong ground motion has been recorded in SMART-1 array, and the site-dependent spectrum has been studied by using these recorded data, hence, for comparison, the paper presented here will be devoted to the study of soil amplification effect theoretically, where the generalized ray theory [2] will be employed to obtain the responses of seismic wave propagating in single layered soil medium overlaying half space. For the simulation of seismic source, the equalvalent shear force is adopted as a source model, then wave from the source can be represented by an integral mathematically, which is known as a ray, and when the wave impinge upon the free surface or interface, it will be transmitted into another medium or reflected back from the boundary, thus, the transmission or reflection coefficients [4] must be considered. Finally, the well-known Cagniard method [5] is used for inverse Laplace transform to save the running time for computer and reduce the numerical error.

GENERALIZED RAY THEORY

A single layered medium overlaying half-space as shown in Fig. 1 is assumed in this study. The material parameters for the upper medium and half space are

respectively denoted by $\rho_1, \mu_1, c_1, C_1, a_1, b_1, \rho_2, \mu_2, c_2, C_2, a_2, b_2$, where ρ is the mass density, μ is shear modulus, c is the compressive wave speed, C is the shear wave speed, $a = 1/c$ is the slowness for compressive wave, whereas $b = 1/C$ is the slowness for shear wave, on which the parameters with subscript "1" and "2" denote those for top layer and half space respectively.

Generalized Ray Integral The Helmholtz decomposition for displacement \vec{u} and body force \vec{F} are respectively written as

$$\vec{u} = \nabla\phi + \nabla \times \vec{\Psi}, \quad \nabla \cdot \vec{\Psi} = 0, \quad (1)$$

$$\vec{F} = \nabla G + \nabla \times \vec{H}, \quad \nabla \cdot \vec{H} = 0, \quad (2)$$

where ϕ and G are the scalar potentials and $\vec{\Psi}$ and \vec{H} are vector potential functions. If we let

$$\vec{\Psi} = 1/r \partial\psi / \partial\theta \vec{e}_r - \partial\psi / \partial r \vec{e}_\theta + \chi \vec{e}_z, \quad (3)$$

$$\vec{H} = 1/r \partial H_2 / \partial\theta \vec{e}_r - \partial H_2 / \partial r \vec{e}_\theta + H_1 \vec{e}_z, \quad (4)$$

then by substituting equation (1), (2), (3) and (4) into Navier's equation, giving

$$c^2 \nabla^2 \phi + G = \partial^2 \phi / \partial t^2, \quad (5)$$

$$C^2 \nabla^2 \psi + H_2 = \partial^2 \psi / \partial t^2, \quad (6)$$

$$C^2 \nabla^2 \chi + H_1 = \partial^2 \chi / \partial t^2, \quad (7)$$

where $\nabla^2 = \partial^2 / \partial r^2 + 1/r \partial / \partial r + 1/r^2 \partial^2 / \partial \theta^2 + \partial^2 / \partial z^2$. If we define Laplace and Hankel transforms to be employed as

$$\bar{\phi}(r, \theta, s) = \int_0^\infty \phi(r, \theta, t) e^{-st} dt, \quad (8)$$

$$\bar{\phi}_n(\xi, \theta, s) = \int_0^\infty \bar{\phi}(r, \theta, s) J_n(s\xi r) r dr, \quad (9)$$

where J_n is the Bessel function of first kind of order n , t denotes time variable and r denotes the epicenter distance. Then for an initially static particle excited by a concentrated body force \vec{F} with acting duration $f(t)$ at a distance z_0 under the interface in a direction $\vec{a} = a_r \vec{e}_r + a_\theta \vec{e}_\theta + a_z \vec{e}_z$, the potential solutions of which are

$$\begin{aligned} \bar{\phi}(r, z, s) = & a_z s^2 \bar{F}(s) \int_0^\infty S_p e^{-s\eta_2 |z-z_0|} J_0(s\xi r) \xi d\xi \\ & + a_r s^2 \bar{F}(s) \int_0^\infty S_p' e^{-s\eta_2 |z-z_0|} J_1(s\xi r) \xi d\xi, \end{aligned} \quad (10)$$

$$\begin{aligned} \bar{\Psi}(r, z, s) = & -a_z s \bar{F}(s) \int_0^\infty S_v e^{-s\zeta_2 |z-z_0|} J_0(s\xi r) d\xi \\ & - a_r s \bar{F}(s) \int_0^\infty S_v' e^{-s\zeta_2 |z-z_0|} J_1(s\xi r) d\xi, \end{aligned} \quad (11)$$

$$\bar{\chi}(r, z, s) = -a_\theta s^2 \bar{F}(s) \int_0^\infty S_h e^{-s\zeta_2 |z-z_0|} J_1(s\xi r) d\xi, \quad (12)$$

where $\bar{F}(s) = \bar{f}(s) / (4\pi\rho_2 s^2)$, $S_p = -\epsilon$, $S_p' = -\xi/\eta_2$, $S_v = \xi/\zeta_2$, $S_v' = \epsilon$, $S_h = 1/(\zeta_2 C_2^2)$, $\epsilon = \text{sgn}(z-z_0)$, $\eta_2 = (\xi^2 + a_2^2)^{1/2}$, $\zeta_2 = (\xi^2 + b_2^2)^{1/2}$, and $\bar{f}(s)$ is the Laplace transform of $f(t)$. From equation (1), (10), (11) and (12), we obtain the horizontal displacement for the concentrated force acting in horizontal direction as

$$\begin{aligned}
\bar{u}_r = & -s^3 \bar{F}(s) \int_0^\infty S_p^i D_{rp} e^{-s\eta_2 |z-z_o|} J_0(s\xi r) \xi d\xi \\
& -s^3 \bar{F}(s) \int_0^\infty S_v^i D_{rv} e^{-s\zeta_2 |z-z_o|} J_0(s\xi r) \xi d\xi \\
& + \frac{s^2}{r} \bar{F}(s) \int_0^\infty S_p^i D_{rp} e^{-s\eta_2 |z-z_o|} J_1(s\xi r) d\xi \\
& + \frac{s^2}{r} \bar{F}(s) \int_0^\infty S_v^i D_{rv} e^{-s\zeta_2 |z-z_o|} J_1(s\xi r) d\xi \\
& + \frac{s^2}{r} \bar{F}(s) \int_0^\infty S_h D_{rh} e^{-s\zeta_2 |z-z_o|} J_1(s\xi r) d\xi
\end{aligned} \tag{13}$$

where $D_{rp} = \eta_2 \xi$, $D_{rv} = -\epsilon \zeta_2$, $D_{rh} = 1$.

As the wave impinge upon the boundary, the impinging point can be treated as a new source and again the wave from the new source will impinge upon another boundary. Hence, the ray integral can be constructed by considering the source function and reflection or transmission coefficients. The following example shows the P-wave, emitted from half space, be transmitted into the upper medium, then after reflected twice it arrive the receiver on surface, of which the ray integral is expressed as

$$(\bar{u}_r)_f = -s^3 \bar{F}(s) \int_0^\infty S_p T_{PS}^{(1)} R_{SS}^{(0)} R_{(1)}^{SP} D_{rp}^f e^{-sh(\xi, z)} J_0(s\xi r) \xi d\xi, \tag{14}$$

where $h(\xi, z) = \eta_2 z_o + 2\zeta_1 + \eta_1 z$, superscript '(0)' means free surface and $R_{SS}^{(0)}$ denotes the reflection coefficient for the incident S-wave reflected as S-wave on the free surface, whereas subscript '(1)', it denotes interface, then $R_{(1)}^{SP}$ denotes the reflection coefficient for the incident S-wave reflected as P-wave on the interface and $T_{PS}^{(1)}$ is that for the incident P-wave transmitted into medium 1 as S-wave. As for the other reflection and transmission coefficients, they can be explained in the same way, and the interested reader can refer to reference [4]. It should be noticed that the receiver function in equation (14) must be modified as follows [2]

$$D_{rp}^f = D_{rp} + R_{PP}^{(0)} D_{rp} + R_{PS}^{(0)} D_{rv}, \quad D_{rp}^i = T_{PP}^{(1)} D_{rp} + T_{PS}^{(1)} D_{rv}, \tag{15}$$

$$D_{rv}^f = D_{rv} + R_{SP}^{(0)} D_{rp} + R_{SS}^{(0)} D_{rv}, \quad D_{rv}^i = T_{SP}^{(1)} D_{rp} + T_{SS}^{(1)} D_{rv}, \tag{16}$$

$$D_{rh}^f = 2, \quad D_{rh}^i = T_H^{(1)}, \tag{17}$$

where the superscript 'f' denotes free surface and 'i' denotes interface.

Hence, if the wave is multiply reflected in surface layer, then the general ray integral for equation (14) can be written as

$$(\bar{u}_r)_f = -s^3 \bar{F}(s) \int_0^\infty S(\xi) \Pi(\xi) D_{rp}^f e^{-sh(\xi, z)} J_0(s\xi r) \xi d\xi, \tag{18}$$

where Π is the product of reflection and transmission coefficients.

At the moment, for an initial static condition, the velocity in Laplace transform can be derived as

$$\bar{v}_r = s \bar{u}_r, \tag{19}$$

Futhermore, the responses for shear force source can be obtained by the following expression

$$\bar{u}_r^s = \frac{\partial \bar{u}_r}{\partial z}, \tag{20}$$

where the superscript 's' denote the shear force source.

Cagniard Method If we express the integral as follows

$$\bar{I}_r(r, z, s) = \int_0^{\infty} E_r(\xi) e^{-sh(\xi, z)} J_0(s\xi r) \xi d\xi, \quad (21)$$

where $E_r(\xi)$ is an even function of ξ , then the inverse of equation (19) can be obtained by convolving $I_r(r, z, t)$ with the inverse of $-s^4 \bar{F}(s)$.

The inverse of equation (21) can be achieved by the well-known Cagniard method. To begin with this work, the Bessel function in equation (21) must be expanded in exponential form, which gives

$$\bar{I}_r(r, z, s) = \frac{2}{\pi} \text{Re} \int_0^{\pi/2} d\omega \int_0^{\infty} E_r(\xi) e^{s g} \xi d\xi, \quad (22)$$

where

$$g(r, z, \xi) = i\xi r \cos \omega - h(\xi, z), \quad (23)$$

if we let

$$-t = g(r, z, \xi), \quad (24)$$

and keep t real and greater than zero, then the inverse of equation (22) can be obtained by observation, that is to say, if we transform equation (22) in ξ -plane into t -plane by virtue of equation (24) as shown in Fig. 2 and 3, it gives

$$\bar{I}_r(r, z, s) = \frac{2}{\pi} \text{Re} \int_0^{\pi/2} d\omega \int_{AB} E_r[\xi(t, \omega)] \xi \left[\frac{\partial \xi}{\partial t} \right]_{\omega} e^{-st} dt, \quad (25)$$

and the inverse of \bar{I}_r is

$$I_r(r, z, s) = H(t-t_m) \frac{2}{\pi} \text{Re} \int_0^{\pi/2} E_r[\xi(t, \omega)] \xi \left[\frac{\partial \xi}{\partial t} \right]_{\omega} d\omega, \quad (26)$$

where $H(t)$ is the Heaviside step function, and t_m is the arrival time, which is obtained by substituting the stationary point ξ_m obtained from $[\partial t / \partial \xi]_{\omega} = 0$ into equation (24).

NUMERICAL RESULTS AND CONCLUSION

The amplification spectra shown in Fig. 4 and 5 [3] were obtained from the data recorded in SMART-1 array on Jan. 16, May 20 and July 30 in the year of 1986 which are hereafter referred to as case I, II and III respectively. As for the epicenter distance and focal depth in case I are respectively 22.2 km and 10.2 km, those for case II are 67.9 km and 15.8 km and for case III they are 5.8 km and 1.6 km. It is found from these figures that the frequency for predominant amplification range from 0.2 Hz to 1.5 Hz.

In order to check the observed velocity amplification spectrum theoretically, the thickness h of the surface layer is assumed 400 m, and the mass density, shear modulus, compressive wave speed and shear wave speed for surface layer and half space are respectively given as $\rho_1 = 1800 \text{ kg/m}^3$, $\mu_1 = 1.023 \times 10^9 \text{ NT/m}^2$, $c_1 = 1900 \text{ m/s}$, $C_1 = 775.67 \text{ m/s}$, $\rho_2 = 2700 \text{ kg/m}^3$, $\mu_2 = 14.4 \times 10^9 \text{ NT/m}^2$, $c_2 = 4000 \text{ m/s}$, $C_2 = 2309.4 \text{ m/s}$, and the distance between the source and the interface are $z_0 = 9.8 \text{ km}$ for case I, $z_0 = 15.4 \text{ km}$ for case II, $z_0 = 1.2 \text{ km}$ for case III.

To simulate the seismic source, the shear force source with sine-like time function

$$\begin{aligned} f(t) &= -P \Delta^{-10} t^{10} + 10P \Delta^{-9} t^9 - 40P \Delta^{-8} t^8 + 80P \Delta^{-7} t^7 \\ &\quad - 80P \Delta^{-6} t^6 + 32P \Delta^{-5} t^5, & 0 \leq t \leq 2\Delta \\ &= 0, & 2\Delta < t \end{aligned}$$

is assumed, where P is the magnitude of the applied force and equals to 10^{15} NT in this case, whereas Δ is half of the applied duration, and we assume $\Delta = 0.2$ sec in this study.

To calculate the total responses, 1364 and 682 rays were respectively considered at the locations on free surface and interface, of which the amplification spectra for case III, I and II are respectively depicted in Fig.6, 7 and 8, then from these figures, we observe that the theoretical fundamental frequency is more closer to that of observed data for case I and II than for case III, this insures us that the ray theory is an useful mathematical tool for the calculation of amplification spectra, furthermore, it suggests that the consideration of finite fault is necessary for the calculation of amplification spectra in near field.

REFERENCES

1. Ceranoglu, A. N., " Acoustic Emission and Propagation of Elastic Pulses in a Plate ", Ph. D. Thesis, Cornell University, Ithaca, New York, 1979.
2. Pao, Y. H. and Gajewski, R. R., " The Generalized Ray theory and Transient Response of Layered Elastic Solids ", Physical Acoustics, Vol. 13, W. P. Mason and R. N. Thurston, eds., Academic Press, New York, 1977, pp. 184-265.
3. Wen, K. L. and Yeh, Y. T., " Effects of Local geology to earthquake records", Proceedings of the Seminar on Geophysics in Taiwan, National Central University, 1986, pp.75-85.
4. Ewing, W. M., Jardetsky, W. S. and Press, F., " Elastic Waves in Layered Media ", Ch. 4, McGraw-Hill, New York, 1957.
5. Cagniard, L., " Reflection and Refraction of Progressive Seismic Waves ", (English translation by E. A. Flynn and C. H. Dix), McGraw-Hill, New York, 1962.

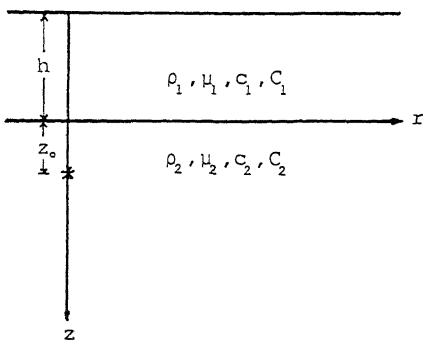


Fig. 1 The geometrical and material parameters for mathematical model under investigation

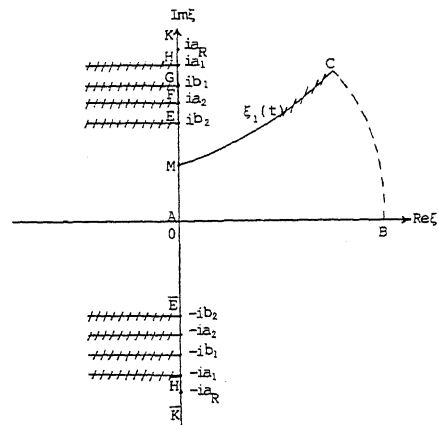


Fig. 2 The ξ -plane in Cagniard method

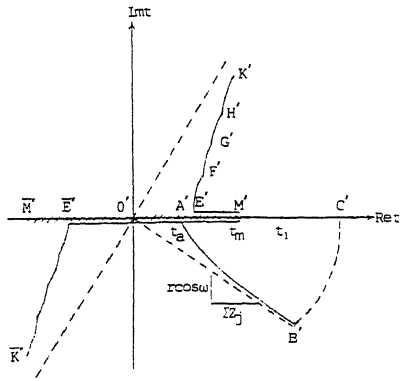


Fig. 3 The t-plane in Cagniard method

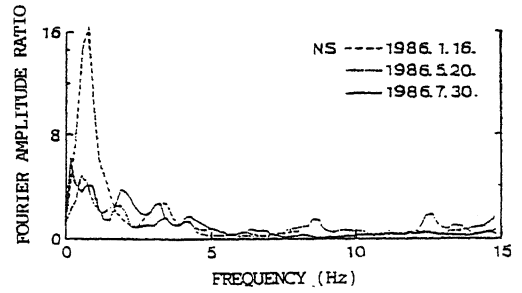


Fig. 4 The NS-direction velocity amplification spectrum in SMART-1 region

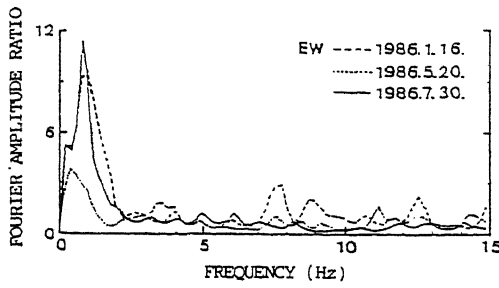


Fig. 5 The EW-direction velocity amplification spectrum in SMART-1 region

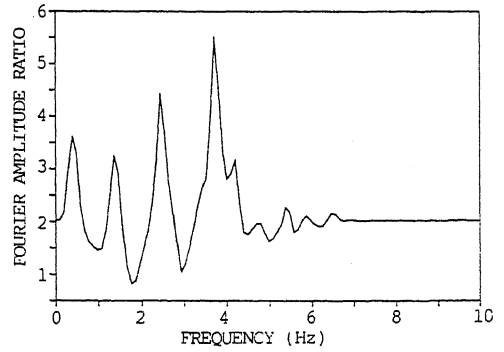


Fig. 6 The velocity amplification spectrum in epicenter distance 5.8 km by generalized ray theory

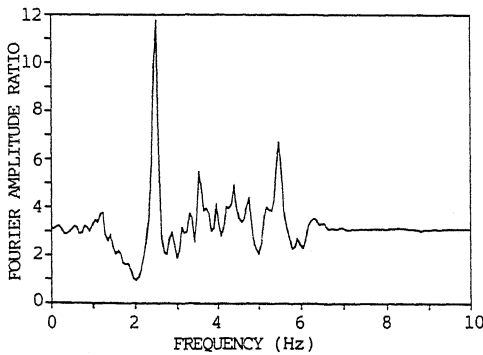


Fig. 7 The velocity amplification spectrum in epicenter distance 22.2 km by generalized ray theory

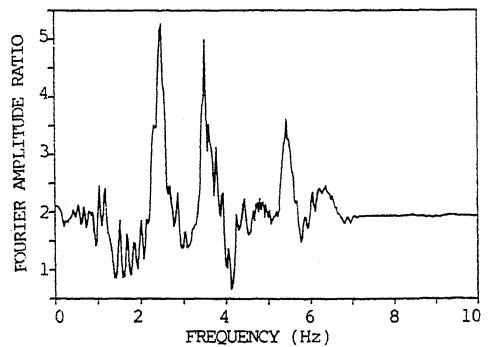


Fig. 8 The velocity amplification spectrum in epicenter distance 67.9 km by generalized ray theory